Extended Benzene-Fused Oligo-BODIPYs: In Three Steps to a Series of Large, Arc-Shaped, Near-Infrared Dyes

Atanu Patra[+], Lukas J. Patalag[+], Peter G. Jones, and Daniel B. Werz*

Dedicated to Professor Henning Hopf on the occasion of his 80th birthday

Abstract: *We present a straightforward, three-step synthesis engaging an oligomerization and subsequent one-pot oxidation step to form fully conjugated, benzene-fused oligo-BODIPYs from simple BODIPY precursors. $FeCl_3$ serves as an efficient, bifunctional oxidant for a (multiple) cyclization/desaturation process, applied to ethylene-bridged dimeric, trimeric and oligomeric species to transform linking ethano units into stiff benzene fusions between unsubstituted β-positions of each BODIPY unit. The structural integrity was verified by X-ray crystallography, and all target compounds were studied in detail by photophysical, electrochemical and computational means. The main S_1 excited state gradually converges to a structure-specific excitation limit, displaying a strong shift of the absorption event from about 500 nm (BODIPY monomer) to 955 nm (octamer) with attenuation coefficients up to ca. 500 000 $M^{-1} cm^{-1}$.*

Although the BODIPY skeleton was first synthesized more than 50 years ago,[1] it has lost neither its fascination for physical-organic chemists nor any of its importance as a dye and fluorophore.[2] Numerous structural modifications of the BODIPY scaffold either at the periphery or by exchanging the substituents at the boron atom have been developed to modify its photophysical properties. Such carefully designed BODIPY derivatives have found applications in biological labelling,[3] photodynamic therapy,[4] tunable laser dyes,[5] emissive materials in OLEDs[6] and organic photovoltaics.[7] A continuing urgent challenge is that of spectrally exploiting

the near infrared (NIR) region by structural fine-tuning that preserves global stability towards multiple excitations and air.[8] While excitonically coupled systems[9] and aggregates[10] present one fruitful direction to achieve that goal, the commonly chosen strategy is to enlarge the π-conjugated scaffold.[11] In general, such an approach lowers the LUMO level whereas the HOMO level may be slightly increased. However, strongly increased HOMO levels should be avoided, otherwise stability might become significantly compromised. Thus, benzene rings have been fused to the pyrrolic moieties[12] or even two BODIPY units connected via additional rings, allowing rigidified π-conjugation. Synthetically, all these so-called "conformation-restricted" BODIPY dimers have been synthesized by preparation of the organic core in a multistep synthesis terminated by complexation of the nitrogen atoms by BF_2 units. Because the synthesis of the nitrogen-containing organic framework is tedious, only dimers of such compounds have been synthesized to date (Scheme 1, top).[13]

Recently, we developed an oxidative approach to access BODIPY oligomers that are linked at their α-positions via ethano units.[14] In an iterative, two-step synthetic protocol starting from the parent BODIPY motif, oligomers up to an octamer species were accessible in reasonable yields. We hypothesized that these compounds might be suitable starting materials to yield extended benzene-fused oligo-BODIPYs (Scheme 1, bottom) by means of a single, additional oxidative step. To connect and rigidify two ethylene-bridged BODIPY units by a shared benzene ring, a dehydrogenative C−C coupling at the β-carbon atoms of the pyrrolic units is necessary, followed by a subsequent dehydrogenation of the ethano unit; thus, in total, four hydrogen atoms need to be removed during this oxidative process. In contrast to previous syntheses of fused BODIPYs, a lengthy multistep synthesis of nitrogen-containing π-systems can be circumvented via a final one-pot, multistep oxidation sequence on pre-assembled ethylene-bridged oligo-BODIPYs.

To test our notion whether such an oxidative approach might be feasible, we tested various oxidation agents for the ethylene-bridged open-chain dimer **2^Op1**. Indeed, the hypervalent iodine reagent PIFA[15] as mild oxidant furnished a cyclized product **2^CyD1** and a corresponding completely oxidized, benzene-fused species **2^D1** in a ratio of ca. 1:2 with re-isolated starting material (Scheme 2). Optimization studies using refined conditions and various hypervalent iodine reagents were unsuccessful. In analogy to the Scholl reaction, which is often employed to access small graphene moieties[16] by oxidative C−C coupling, we switched to the one-electron

[*] Dr. A. Patra,[+] Dr. L. J. Patalag,[+] Prof. Dr. D. B. Werz
Technische Universität Braunschweig
Institute of Organic Chemistry
Hagenring 30, 38106 Braunschweig (Germany)
E-mail: d.werz@tu-braunschweig.de
Homepage: http://www.werzlab.de

Prof. Dr. P. G. Jones
Technische Universität Braunschweig
Institute of Inorganic and Analytical Chemistry
Hagenring 30, 38106 Braunschweig (Germany)

[+] These authors contributed equally to this work.

Supporting information and the ORCID identification number(s) for the author(s) of this article can be found under:
https://doi.org/10.1002/anie.202012335.
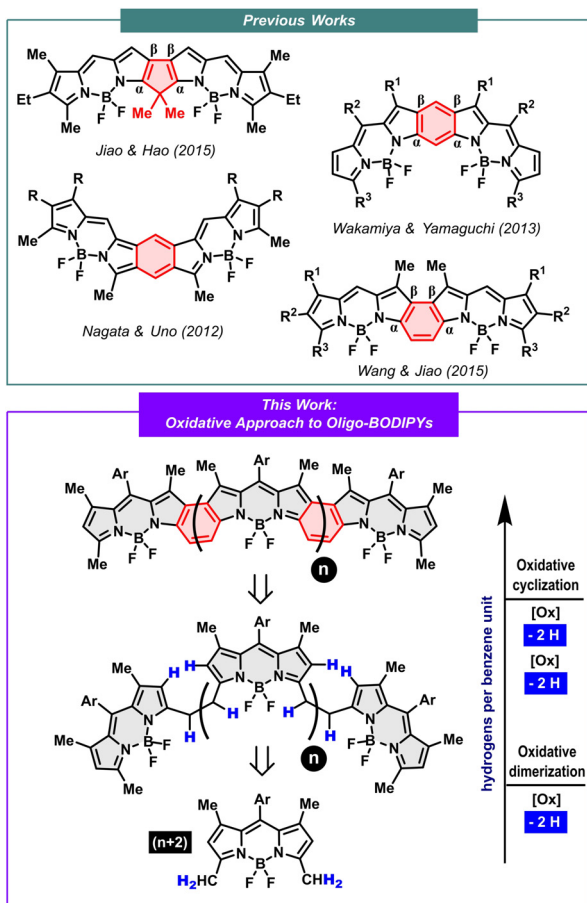
Scheme 1. Several π-conjugated BODIPY dimers (top) and our approach to access fully conjugated, benzene-fused BODIPY oligomers.

Figure 1. Molecular structures of dimer 2^{D2} and trimer 3^{T2} and selected bond lengths and distances (rounded) of 2^{D2}, 2^{CyD2} and 3^{T2} obtained by X-ray diffraction analyses.[20] *Meso* group Ar^2 truncated for simplicity. For geometry of 2^{CyD2} and exact values see the Supporting Information.

oxidant FeCl$_3$,[17] which gave excellent yields of the benzene-fused dimer 2^{D1} of up to 95% in DCM when nitromethane was employed as a necessary co-solvent.[13d] A deeper investigation revealed that both a large excess of FeCl$_3$ and a carefully gauged reaction time are essential. The latter condition results from the fact that in situ generated HCl is detrimental to all reaction intermediates and is able to initiate various decomposition pathways such as the decomplexation of BF$_2$ units. However, the addition of a neutralizing base was unrewarding and shut down the transformation completely. With specifically adjusted reaction conditions in hand, corresponding benzene-fused trimers 3^{T1} and 3^{T2} were obtained in 62% and 51% yield, respectively, assigning the *meso* group as a non-participating residue. The fully conjugated benzene-fused tetramer **4**, hexamer **6** and octamer **8** were finally isolated in 42%, 25% and 19% yield as uniformly blue-colored solids with no signs of decomposition under air. Single crystal X-ray diffraction revealed the exact geometries of the cyclized dimer 2^{CyD2}, the benzene-fused dimer 2^{D2} and the trimer 3^{T2} (Figure 1) in the solid state. As suggested by the structural formulae of 2^{D2} and 3^{T2}, the bond lengths within the benzene rings are not uniform; the unsaturated bond at the former ethano unit is much shorter (1.36–1.37 Å) than its adjacent double bonds (1.42–1.45 Å).
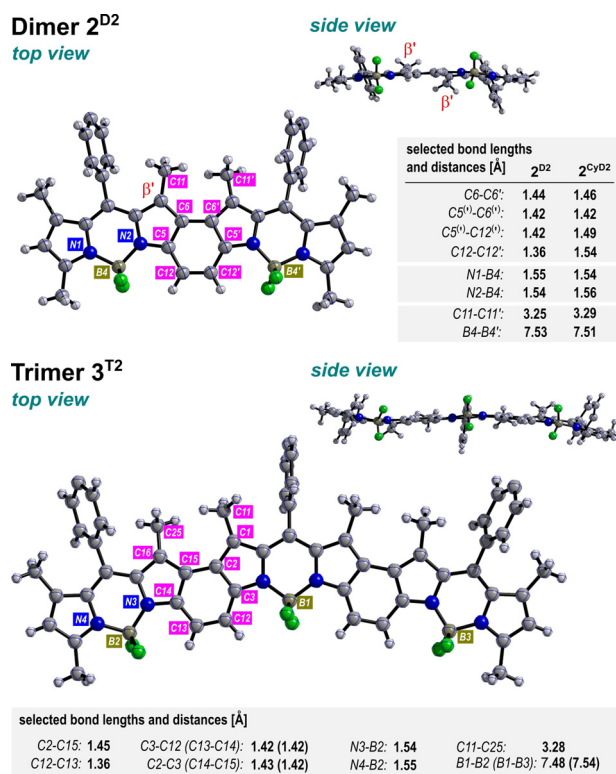
Compared to the cyclized dimer 2^{CyD2}, the additional unsaturation of 2^{D2} contracts the close vicinity of the BF$_2$ units. All structures are characterized by an impaired planarity as consequence of the inner β′-pyrrolic methyl groups, which tend to avoid each other through steric repulsion, thus defining local C_2 axes at these positions. We estimated the energy barrier of this local atropisomerism computationally via a quasi-planar transition state and obtained a low value of $\Delta G^{\ddagger} \approx 2$ kcal mol^{-1}. The B−N bonds lie in the normal range for BODIPYs (1.53–1.55 Å).

For a first photophysical investigation, steady-state absorption and emission spectra were recorded in DCM, THF and toluene (see Figure 2). The benzene-fused dimerization of a BODIPY monomer results in a strong bathochromic shift of ca. 140 nm (ca. 4000 cm^{-1}) regarding the main absorption and emission band. The shift is accompanied by a pronounced vibronic progression, which is however mitigated when the central benzene ring is saturated, as in 2^{CyD1} (see the Supporting Information). The Stokes shift of dimer 2^{CyD1} is also consistently higher than for its benzene-fused congener, indicating a higher degree of geometrical reorganization in S$_1$ based on the reduced coplanarity and rigidity of the sole β–β conjugation. Interestingly, while the squared transition dipole moment $(\mu_{eg})^2$ of the cyclized dimer 2^{CyD1} is roughly the sum of two BODIPY monomers (see Table 1), the benzene fusion strongly increases the intrachromophoric coupling leading to a ca. 3.5-fold rise in $(\mu_{eg})^2$. This manifests itself in a higher attenuation coefficient of 2^{D1}, while the value
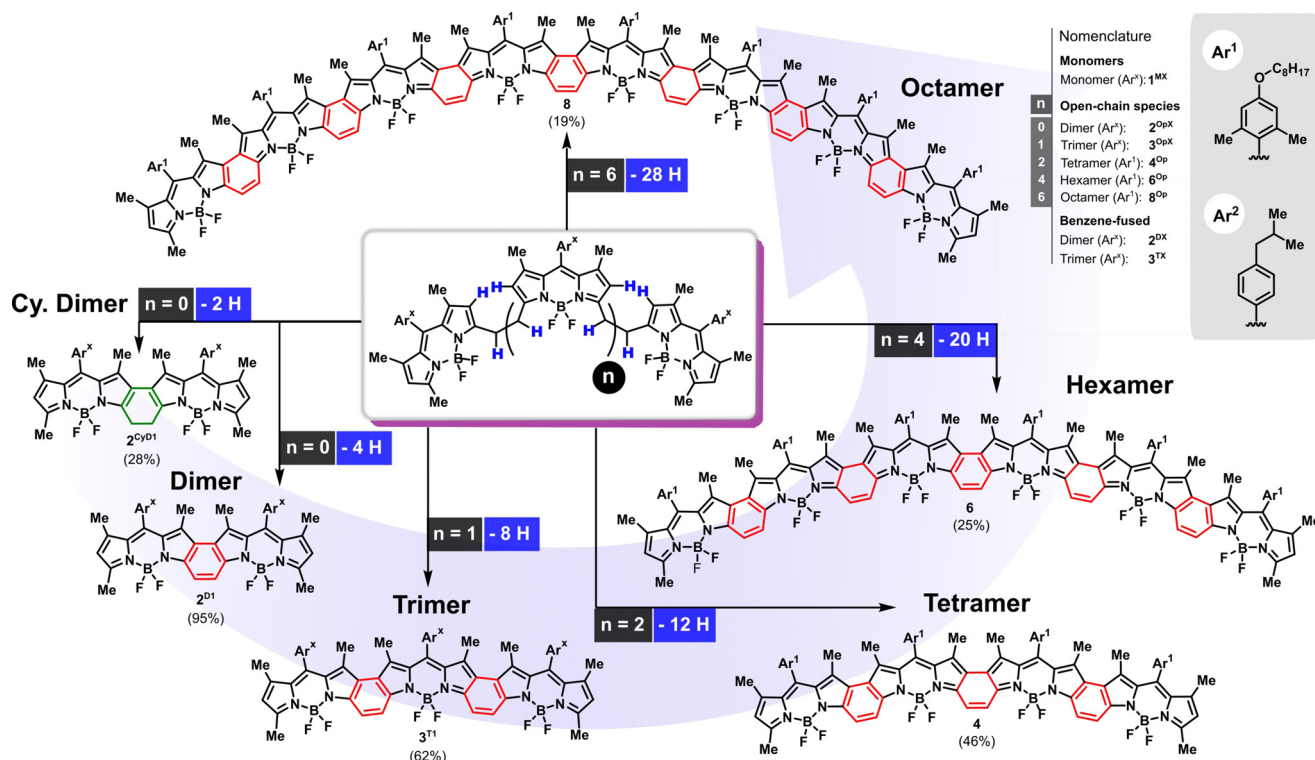
Scheme 2. Synthetic Scheme to the entire series of oligo-BODIPYs, focusing on the yields with *meso* substituent Ar¹, starting from the corresponding open-chain species. All reactions are carried out with customized amounts of FeCl₃ in a DCM/MeNO₂ solvent system (see Supporting Information), except for **2^CyD1**, for which PIFA/BF₃·OEt₂ was used as oxidant.

of the cyclized counterpart only slightly surpasses its BODIPY precursor. Cyclized dimer **2^CyD1** might thus also be regarded as an intramolecular J-aggregate in the strong coupling regime. Both attenuation coefficients are highest in toluene and only weakly reduced by increasing solvent polarity. As anticipated, the second red-shift of the trimer species is significantly less pronounced (ca. 115 nm, 2400 cm⁻¹) and the fluorescence quantum yield drops dramatically ($\Phi_\mathrm{F} = 0.07$/THF and 0.13/toluene). For the tetramer,

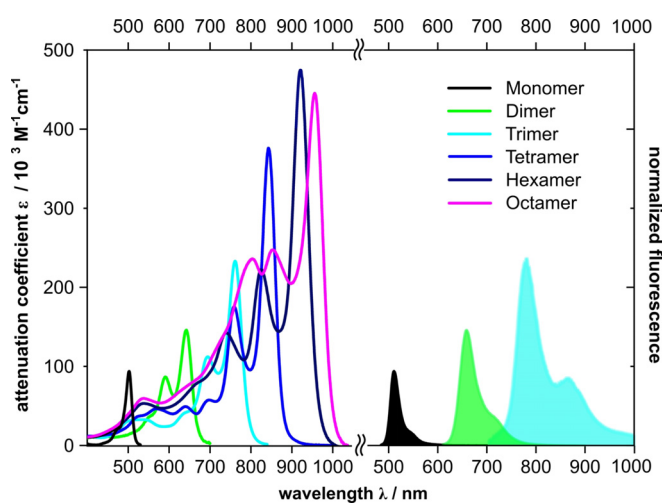hexamer and octamer congeners an emission was virtually undetectable. This decrease is more drastic than the theoret-

Table 1: Selection of spectroscopic data.

(oligo-)BODIPY	$\lambda^{A[a]}$	$\lambda^{F[b]}$	$\Delta\tilde{\nu}^{[c]}$	$\varepsilon^{[d]}$	$\Phi_\mathrm{F}^{[e]}$	$f^{[f]}$	$(\mu_\mathrm{eg})^{2[g]}$
Monomer	503	511	312	94	0.92	0.43	36
	504	*513*	*348*	*99*	*0.94*	*0.44*	*35*
Dimer	*636*	*658*	*525*	*98*	*0.51*	*0.76*	*79*
(cycl./2^CyD1)	*644*	*663*	*445*	*109*	*0.60*	*0.79*	*78*
Dimer	642	658	378	146	0.42	1.31	128
	651	*664*	*301*	*160*	*0.62*	*1.31*	*121*
Trimer	761	780	320	233	0.07	1.58	191
	767	*780*	*217*	*267*	*0.13*	*1.57*	*182*
Tetramer	841	n.d.[h]	–	330	n.d.[h]	2.07	293
	842			*376*		*2.12*	*281*
Hexamer	921	n.d.[h]	–	475	n.d.[h]	3.36	473
	922			*529*		*3.25*	*438*
Octamer	955	n.d.[h]	–	446	n.d.[h]	4.14	590
	957			*454*		*3.77*	*508*

First value in DCM, second value in toluene (underlined) for series with Ar¹ *meso* group. For full data (THF, lifetimes etc.) see the Supporting Information. [a] Main, lowest energy absorption band [nm]. [b] Main, highest energy fluorescence band [nm]. [c] Stokes shift [cm⁻¹]. [d] Attenuation coefficient [10³ M⁻¹ cm⁻¹]. [e] Absolute fluorescence quantum yield at rt. [f] Oscillator strength according to equation S1. [g] Squared transition dipole moment [D²] referring to the S₁ excited state according to equation S2. [f,g] Integral barriers for trimer, tetramer, hexamer and octamer are only estimated, because of a second overlapping absorption band. [h] n.d. = not detected.

Figure 2. Absorption and emission spectra of the benzene-fused oligo-BODIPY series with Ar¹ *meso* substituent in DCM at rt.

ical prediction by the *energy gap rule*. TDDFT computations assign a dominating HOMO→LUMO contribution to the main S_1 excited state; this is consistently true for all benzene-fused oligomeric species presented here (see the Supporting Information). For species with an even number of BF_2 units, the HOMO is of B_1 and the LUMO of A_2 pseudosymmetry, respectively, while the opposite is true for the cases with an odd number of BODIPY subunits. Consequently, this transition is highly symmetry-allowed, which explains the strong absorptions detected and the gradually thwarted red-shift as a result of the converging HOMO–LUMO energy gap (see Figure 3 C). Remarkably, the frontier orbitals evolve a distinctly shaped super-pattern with repetitive localizations of electron density (see Figure 3 A). For instance, while the electron density of the HOMO–LUMO pair accumulates at the respective geometrical centers, their frontier orbital homologs localize in a wave-like fashion occupying also geometrical termini (see HOMO−1). Along the growing oligomers within the series, the contribution of frontier orbital homologs to S_1 clearly gains relevance according to our TDDFT results and evolves a detrimental effect for a preferably undisplaced S_1 potential energy surface. We thus hypothesize that the increasing orbital mixing and impaired

orbital co-localization compromises high Franck-Condon factors necessary for an efficient radiative decay, which appears consistent with the rapid loss of emission quality in larger species.

Finally, we attempted to simulate the spectral evolvement of the absorption bands by two computational approaches (see Figure 3 D). As anticipated, TDDFT consistently overestimates the main excitation energy, by an approximately constant error of ca. 0.4 eV. This discrepancy is widely known in the literature[18] and might be interpreted as a proof of an inherent cyanine-quality of the oscillating π-systems. The novel DLPNO-STEOM-CCSD approach of the Neese group,[19] which was only applied to the monomeric and dimeric species because of computational expense, was able to achieve a much higher accuracy with a slight underestimation of the lowest-energy excitation event (by less than 0.1 eV).

Figure 4 depicts the cyclic voltammograms of the entire oligo-BODIPY series, which were recorded in DCM with nBu_4NPF_6 as supporting electrolyte without indication of any change or decomposition at slow scan rates. The number of chemically reversible reduction potentials gradually increases with the number of integrated benzene/BODIPY subunits. However, since the unoccupied frontier orbitals quickly converge along the oligomeric series, the reduction waves start to overlap in a similar manner, making single peaks hard to distinguish by common cyclovoltammetry.

The grey dots nicely illustrate this convergence towards a motif-dependent LUMO energy limit. On the oxidation side, the main quasi-reversible oxidation wave first undergoes a significant shift towards a lower potential (monomer to dimer), but afterwards levels off within a narrow potential window for the higher homologs, which underlines the widely unchanged HOMO energy. Similarly to the reduction behavior, additional oxidation waves start to emerge along the series, but quickly merge with the main lowest-potential wave. Only for the trimer case does a second oxidation wave appear well-resolved.
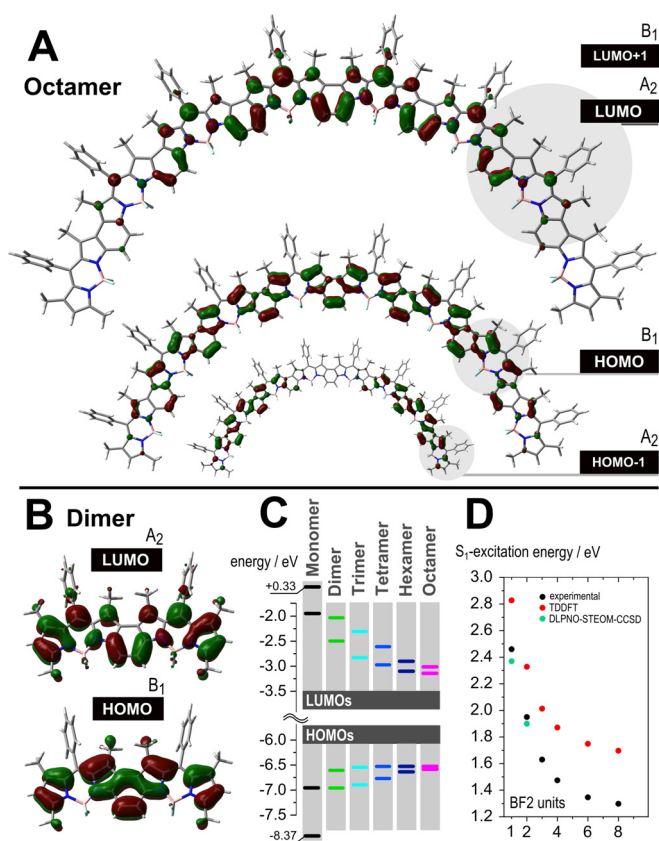

Figure 3. Computational results, DFT: M052X-D3/Def2-SVP/DCM-(PCM), TDDFT: M052X-D3/Def2-TZVP/DCM(PCM). A) Frontier orbitals of a prototypical octamer species (simplified *meso* substituent) and their pseudosymmetries. B) Frontier orbitals of a corresponding benzene-fused dimer species. C) Schematic evolvement of frontier orbital energies (DFT). D) Comparison of experimental and theoretical excitation energies.
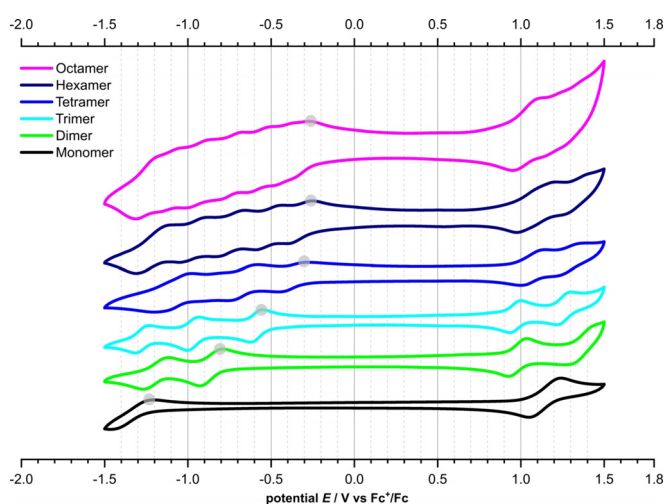

Figure 4. Cyclic voltammograms of monomer **1M**[1] and its benzene-fused oligomeric congeners with Ar[1] *meso* group. Recorded in DCM at rt versus Fc[+]/Fc.

In conclusion, we have presented a straightforward and efficient, oxidative strategy for accessing extended benzene-fused oligo-BODIPYs in only three synthetic steps. An initial oxidative oligomerization protocol provides ethano-linked oligomers from simple α,α′-dimethylated BODIPY precursors. These open-chain substrates are oxidized by FeCl$_3$, initially to create a cyclizing linkage between the β-positions of the pyrrolic subunits and then to dehydrogenate and transform the ethano tethers into multiple benzene-fusions in an effortless, one-pot procedure. Oligomers of up to eight BODIPY subunits with seven linking benzene rings are thereby accessible and develop a distinct arc-shaped morphology. In line with a converging red-shift along the series, which reaches an absorption maximum at 955 nm (DCM) for the octamer species, cyclic voltammetry experiments underpin a converging LUMO energy limit and indicate an excellent robustness towards reversible reduction and oxidation cycles. In addition to the advantageous air stability of all benzene-fused species herein, these results suggest that stable radical monoanions, dianions or even radical trianions might be accessible for higher homologs and be of potential interest for optoelectronic devices which rely on reversible charge separation and transfer.

Acknowledgements

Conflict of interest

The authors declare no conflict of interest.

Keywords: BODIPY · dyes · fluorophores · NIR · π-systems

[1] A. Treibs, F.-H. Kreuzer, *Justus Liebigs Ann. Chem.* **1968**, *718*, 208–223.

[2] a) A. Harriman, G. Izzet, R. Ziessel, *J. Am. Chem. Soc.* **2006**, *128*, 10868–10875; b) A. Loudet, K. Burgess, *Chem. Rev.* **2007**, *107*, 4891–4932; c) L. Li, J. Han, B. Nguyen, K. Burgess, *J. Org. Chem.* **2008**, *73*, 1963–1970; d) G. Ulrich, R. Ziessel, A. Harriman, *Angew. Chem. Int. Ed.* **2008**, *47*, 1184–1201; *Angew. Chem.* **2008**, *120*, 1202–1219; e) D. Frath, J. Massue, G. Ulrich, R. Ziessel, *Angew. Chem. Int. Ed.* **2014**, *53*, 2290–2310; *Angew. Chem.* **2014**, *126*, 2322–2342; f) T. Bruhn, G. Pescitelli, S. Jurinovich, A. Schaumlöffel, F. Witterauf, J. Ahrens, M. Bröring, G. Bringmann, *Angew. Chem. Int. Ed.* **2014**, *53*, 14592–14595; *Angew. Chem.* **2014**, *126*, 14821–14824; g) E. Palao, T. Slanina, L. Muchová, T. Šolomek, L. Vítek, P. Klán, *J. Am. Chem. Soc.* **2016**, *138*, 126–133; h) M. A. Filatov, S. Karuthedath, P. M. Polestshuk, H. Savoie, K. J. Flanagan, C. Sy, E. Sitte, M. Telitchko, F. Laquai, R. W. Boyle, M. O. Senge, *J. Am. Chem. Soc.* **2017**, *139*, 6282–6285; i) J. A. Peterson, C. Wijesooriya, E. J. Gehrmann, K. M. Mahoney, P. P. Goswami, T. R. Albright, A. Syed, A. S. Dutton, E. A. Smith, A. H. Winter, *J. Am. Chem. Soc.* **2018**, *140*, 7343–7346; j) T. Kim, Z. Duan, S. Talukdar, C. Lei, D. Kim, J. L. Sessler, T. Sarma, *Angew. Chem. Int. Ed.* **2020**, *59*, 13063–13070; *Angew. Chem.* **2020**, *132*, 13163–13170.

[3] a) R. E. Pagano, O. C. Martin, H. C. Kang, R. P. Haugland, *J. Cell. Biol.* **1991**, *113*, 1267–1279; b) I. D. Johnson, H. C. Kang, R. P. Haugland, *Anal. Biochem.* **1991**, *198*, 228–237; c) M. L. Metzker, J. Lu, R. A. Gibbs, *Science* **1996**, *271*, 1420–1422; d) S. Kurata, T. Kanagawa, K. Yamada, M. Torimura, T. Yokomaku, Y. Kamagata, R. Kurane, *Nucleic Acids Res.* **2001**, *29*, 34e–38e; e) T. Myochin, K. Hanaoka, T. Komatsu, T. Terai, T. Nagano, *J. Am. Chem. Soc.* **2012**, *134*, 13730–13737; f) L. Wang, Y. Xiao, W. Tian, L. Deng, *J. Am. Chem. Soc.* **2013**, *135*, 2903–2906; g) F. Wang, Y. Zhu, L. Zhou, L. Pan, Z. Cui, Q. Fei, S. Luo, D. Pan, Q. Huang, R. Wang, C. Zhao, H. Tian, C. Fan, *Angew. Chem. Int. Ed.* **2015**, *54*, 7349–7353; *Angew. Chem.* **2015**, *127*, 7457–7461; h) C. S. Wijesooriya, J. A. Peterson, P. Shrestha, E. J. Gehrmann, A. H. Winter, E. A. Smith, *Angew. Chem. Int. Ed.* **2018**, *57*, 12685–12689; *Angew. Chem.* **2018**, *130*, 12867–12871; i) S. Jeon, T.-I. Kim, H. Jin, U. Lee, J. Bae, J. Bouffard, Y. Kim, *J. Am. Chem. Soc.* **2020**, *142*, 9231–9239.

[4] a) S. H. Lim, C. Thivierge, P. Nowak-Sliwinska, J. Han, H. v. d. Bergh, G. Wagnières, K. Burgess, H. B. Lee, *J. Med. Chem.* **2010**, *53*, 2865–2874; b) A. Kamkaew, S. H. Lim, H. B. Lee, L. V. Kiew, L. Y. Chung, K. Burgess, *Chem. Soc. Rev.* **2013**, *42*, 77–88; c) S. Kolemen, M. Işik, G. M. Kim, D. Kim, H. Geng, M. Buyuktemiz, T. Karatas, X.-F. Zhang, Y. Dede, J. Yoon, E. U. Akkaya, *Angew. Chem. Int. Ed.* **2015**, *54*, 5340–5344; *Angew. Chem.* **2015**, *127*, 5430–5434; d) M. Üçüncü, E. Karakuş, E. K. Demirci, M. Sayar, S. Dartar, M. Emrullahoğlu, *Org. Lett.* **2017**, *19*, 2522–2525; e) X. Dai, X. Chen, Y. Zhao, Y. Yu, X. Wei, X. Zhang, C. Li, *Biomacromolecules* **2018**, *19*, 141–149; f) H. Wang, W. Zhao, X. Liu, S. Wang, Y. Wang, *ACS Appl. Bio Mater.* **2020**, *3*, 593–601.

[5] a) M. Shah, K. Thangaraj, M.-L. Soong, L. T. Wolford, J. H. Boyer, *Heteroat. Chem.* **1990**, *1*, 389–399; b) F. López Arbeloa, J. B. Prieto, V. M. Martinez, T. A. Lopez, I. L. Arbeloa, *ChemPhysChem* **2004**, *5*, 1762–1771; c) M. J. Ortiz, I. Garcia-Moreno, A. R. Agarrabeitia, G. Duran-Sampedro, A. Costela, R. Sastre, F. L. Arbeloa, J. B. Prietod, I. L. Arbeloa, *Phys. Chem. Chem. Phys.* **2010**, *12*, 7804–7811; d) M. E. Pérez-Ojeda, C. Thivierge, V. Martín, Á. Costela, K. Burgess, I. García-Moreno, *Opt. Mater. Express* **2011**, *1*, 243–251.

[6] a) L. Bonardi, H. Kanaan, F. Camerel, P. Jolinat, P. Retailleau, R. Ziessel, *Adv. Funct. Mater.* **2008**, *18*, 401–413; b) C. L. Liu, Y. Chen, D. P. Shelar, C. Li, G. Cheng, W. F. Fu, *J. Mater. Chem. C* **2014**, *2*, 5471–5478; c) M. Chapran, E. Angioni, N. J. Findlay, B. Breig, V. Cherpak, P. Stakhira, T. Tuttle, D. Volyniuk, J. V. Grazulevicius, Y. A. Nastishin, O. D. Lavrentovich, P. J. Skabara, *ACS Appl. Mater. Interfaces* **2017**, *9*, 4750–4757; d) H. Gao, Y. Gao, C. Wang, D. Hu, Z. Xie, L. Liu, B. Yang, Y. Ma, *ACS Appl. Mater. Interfaces* **2018**, *10*, 14956–14965.

[7] a) D. Kumaresan, R. P. Thummel, T. Bura, G. Ulrich, R. Ziessel, *Chem. Eur. J.* **2009**, *15*, 6335–6339; b) N. Boens, V. Leen, W. Dehaen, *Chem. Soc. Rev.* **2012**, *41*, 1130–1172; c) T. Kowada, H. Maeda, K. Kikuchi, *Chem. Soc. Rev.* **2015**, *44*, 4953–4972; d) J. J. Chen, S. M. Conron, P. Erwin, M. Dimitriou, K. McAlahney, M. E. Thompson, *ACS Appl. Mater. Interfaces* **2015**, *7*, 662–669; e) R. Mishra, B. Basumatary, R. Singhal, G. D. Sharma, J. Sankar, *ACS Appl. Mater. Interfaces* **2018**, *10*, 31462–31471.

[8] a) K. Umezawa, Y. Nakamura, H. Makino, D. Citterio, K. Suzuki, *J. Am. Chem. Soc.* **2008**, *130*, 1550–1551; b) L. J. Patalag, P. G. Jones, D. B. Werz, *Angew. Chem. Int. Ed.* **2016**, *55*, 13340–13344; *Angew. Chem.* **2016**, *128*, 13534–13539; c) L. J. Patalag, P. G. Jones, D. B. Werz, *Chem. Eur. J.* **2017**, *23*, 15903–15907; d) L. J. Patalag, M. Loch, P. G. Jones, D. B. Werz, *J. Org. Chem.* **2019**, *84*, 7804–7814.

[9] C. Lambert, T. Scherpf, H. Ceymann, A. Schmiedel, M. Holzapfel, *J. Am. Chem. Soc.* **2015**, *137*, 3547–3557.

[10] Z. Chen, Y. Liu, W. Wagner, V. Stepanenko, X. Ren, S. Ogi, F. Würthner, *Angew. Chem. Int. Ed.* **2017**, *56*, 5729 – 5733; *Angew. Chem.* **2017**, *129*, 5823 – 5827.

[11] M. Müller, S. Maier, O. Tverskoy, F. Rominger, J. Freudenberg, U. H. F. Bunz, *Angew. Chem. Int. Ed.* **2020**, *59*, 1966 – 1969; *Angew. Chem.* **2020**, *132*, 1982 – 1985.

[12] a) Y. Hayashi, N. Obata, M. Tamaru, S. Yamaguchi, Y. Matsuo, A. Saeki, S. Seki, Y. Kureishi, S. Saito, S. Yamaguchi, H. Shinokubo, *Org. Lett.* **2012**, *14*, 866 – 869; b) Z. Zhou, J. Zhou, L. Gai, A. Yuan, Z. Shen, *Chem. Commun.* **2017**, *53*, 6621 – 6624; c) W. Miao, Y. Feng, Q. Wu, W. Sheng, M. Li, Q. Liu, E. Hao, L. Jiao, *J. Org. Chem.* **2019**, *84*, 9693 – 9704; d) H. Ito, H. Sakai, Y. Suzuki, J. Kawamata, T. Hasobe, *Chem. Eur. J.* **2020**, *26*, 316 – 325; e) J. Labella, G. Durán-Sampedro, M. V. Martínez-Díaz, T. Torres, *Chem. Sci.* **2020**, *11*, 10778 – 10785.

[13] a) M. Nakamura, H. Tahara, K. Takahashi, T. Nagata, H. Uoyama, D. Kuzuhara, S. Mori, T. Okujima, H. Yamada, H. Uno, *Org. Biomol. Chem.* **2012**, *10*, 6840 – 6849; b) A. Wakamiya, T. Murakami, S. Yamaguchi, *Chem. Sci.* **2013**, *4*, 1002 – 1007; c) M. Nakamura, M. Kitatsuka, K. Takahashi, T. Nagata, S. Mori, D. Kuzuhara, T. Okujima, H. Yamada, T. Nakae, H. Uno, *Org. Biomol. Chem.* **2014**, *12*, 1309 – 1317; d) C. Yu, L. Jiao, T. Li, Q. Wu, W. Miao, J. Wang, Y. Wei, X. Mu, E. Hao, *Chem. Commun.* **2015**, *51*, 16852 – 16855; e) J. Wang, Q. Wu, S. Wang, C. Yu, J. Li, E. Hao, Y. Wei, X. Mu, L. Jiao, *Org. Lett.* **2015**, *17*, 5360 – 5363.

[14] L. J. Patalag, L. P. Ho, P. G. Jones, D. B. Werz, *J. Am. Chem. Soc.* **2017**, *139*, 15104 – 15113.

[15] a) T. Dohi, M. Ito, K. Morimoto, M. Iwata, Y. Kita, *Angew. Chem. Int. Ed.* **2008**, *47*, 1301 – 1304; *Angew. Chem.* **2008**, *120*, 1321 – 1324; b) E. Faggi, R. M. Sebastián, R. Pleixats, A. Vallribera, A. Shafir, A. Rodríguez-Gimeno, C. R. de Arellano, *J. Am. Chem. Soc.* **2010**, *132*, 17980 – 17982.

[16] a) F. Dötz, J. D. Brand, S. Ito, L. Gherghel, K. Müllen, *J. Am. Chem. Soc.* **2000**, *122*, 7707 – 7717; b) F. Schlütter, T. Nishiuchi, V. Enkelmann, K. Müllen, *Angew. Chem. Int. Ed.* **2014**, *53*, 1538 – 1542; *Angew. Chem.* **2014**, *126*, 1564 – 1568; c) A. Narita, X.-Y. Wang, X. Feng, K. Müllen, *Chem. Soc. Rev.* **2015**, *44*, 6616 – 6643; d) J. Liu, A. Narita, S. Osella, W. Zhang, D. Schollmeyer, D. Beljonne, X. Feng, K. Müllen, *J. Am. Chem. Soc.* **2016**, *138*, 2602 – 2608; e) H. Ito, K. Ozaki, K. Itami, *Angew. Chem. Int. Ed.* **2017**, *56*, 11144 – 11164; *Angew. Chem.* **2017**, *129*, 11296 – 11317.

[17] A. B. Nepomnyashchii, M. Bröring, J. Ahrens, A. J. Bard, *J. Am. Chem. Soc.* **2011**, *133*, 8633 – 8645.

[18] a) R. Send, O. Valsson, C. Filippi, *J. Chem. Theory Comput.* **2011**, *7*, 444 – 455; b) B. Le Guennic, D. Jacquemin, *Acc. Chem. Res.* **2015**, *48*, 530 – 537.

[19] R. Berraud-Pache, F. Neese, G. Bistoni, R. Izsák, *J. Chem. Theory Comput.* **2020**, *16*, 564 – 575.

[20] Deposition Number(s) 1563278 (for **2^D2**), 1563277 (for **2^CyD2**), and 2027693 (for **3^T2**) contain(s) the supplementary crystallographic data for this paper. These data are provided free of charge by the joint Cambridge Crystallographic Data Centre and Fachinformationszentrum Karlsruhe Access Structures service www.ccdc.cam.ac.uk/structures.